Composites: Part B 43 (2012) 2298–2302

Contents lists available at SciVerse ScienceDirect

Composites: Part B

journal homepage: www.elsevier.com/locate/compositesb

Effects of silane-modified carbon nanotubes on flexural and fracture behaviors of carbon nanotube-modified epoxy/basalt composites

M.T. Kim [a], K.Y. Rhee [b,*], S.J. Park [c,*], D. Hui [b,d]

[a] Gumi Electronics & Information Technology Research Institute, Gumi 730-853, Republic of Korea
[b] School of Mechanical Engineering, Kyung Hee University, Yongin 446-701, Republic of Korea
[c] Department of Chemistry, Inha University, 253, Nam-gu, Incheon 402-751, Republic of Korea
[d] Department of Mechanical Engineering, University of New Orleans, LA 70148, United States

ARTICLE INFO

Article history:
Received 23 August 2011
Accepted 19 December 2011
Available online 11 January 2012

Keywords:
A. Polymer–matrix composites
B. Mechanical properties
E. Surface treatments

ABSTRACT

We investigated the effects of carbon nanotube (CNT) modification with silane on the flexural and fracture behaviors of modified carbon nanotube epoxy/basalt (CNT/epoxy/basalt) composites. Flexural and mode I fracture tests were performed using acid-treated and silane-treated CNT/epoxy/basalt composites, respectively. FT-IR analysis was conducted to determine the chemical change on the surface of basalt fiber due to the silane modification. After the fracture tests, the fracture surfaces of the CNT/epoxy/basalt composites were examined with scanning electron microscopy (SEM) to investigate the fracture mechanisms of the CNT/epoxy/basalt composites, depending on the CNT modification. The results show that the flexural modulus and strength of silane-treated CNT/epoxy/basalt composites are ~10% and ~14% greater, respectively, than those of acid-treated CNT/epoxy/basalt composites. The fracture toughness G_{Ic} of silane-treated CNT/epoxy/basalt composites was ~40% greater than that of acid-treated CNT/epoxy/basalt composites. SEM examination revealed that the improvement in the flexural and fracture properties of silane-treated CNT/epoxy/basalt composites occurred due to enhanced dispersion and interfacial interaction between the silane-modified CNTs and the epoxy.

© 2012 Elsevier Ltd. All rights reserved.

1. Introduction

Basalt fiber, which is made from basalt rock, exhibits superior thermal performance, mechanical strength, and chemical resistance. Furthermore, basalt fiber can be produced at a considerably lower cost than carbon fiber. For this reason, a number of studies have been performed to investigate the mechanical behaviors of basalt fiber-reinforced composites [1–4].

Carbon nanotubes (CNTs) have remarkable mechanical, electrical, thermal, and many other unique characteristics, allowing them to be used as multi-functional reinforcement materials within polymer matrixes. Accordingly, many studies have been conducted to characterize the mechanical and electrical properties of CNT-reinforced polymer composites [5–11].

Many researchers recently reported that multi-scale composites composed of a mixture of micro-scale fibers and a nano-scale CNT-reinforced polymer matrix synergize mechanical properties better than typical fiber/polymer composites [12–17]. For example, Bekyarova et al. [18] reported that CNT/carbon fabric/epoxy composites enhanced interlaminar shear strength by ~30% compared to that of carbon fiber/epoxy composites without CNTs and significantly improved the out-of-plane electrical conductivity. Qiu et al. [19] reported that the tensile strength and Young's modulus of CNT/glass fabric/epoxy composites increased by 14% and 20%, respectively, in comparison with those of conventional epoxy/glass fiber composites. They also reported that the shear strength and short-beam modulus increased by 5% and 8%, respectively.

CNTs are generally agglomerated and hydrophobic, resulting in degradation of the material properties of CNT-reinforced multi-scale composites. To address this, various dispersion methods such as ultrasonication, chemical functionalization, and mechanical grinding of CNTs have been conducted [20–21]. Lee et al. [22] investigated the effect of silane treatment of CNTs on the tensile properties of CNT/epoxy/basalt multi-scale composites and reported that the tensile strength and Young's modulus of the silane-treated CNT/epoxy/basalt multi-scale composites were ~17% and ~21% greater than those of the acid-treated CNT/epoxy/basalt multi-scale composites, respectively. However, no research result has been reported on the effect of silane treatment of CNTs on the fracture behaviors of CNT/epoxy/basalt multi-scale composites.

In the present study, CNTs were surface-treated with silane to improve dispersion and their interfacial strength with the epoxy matrix, and the treatment effects on the flexural and mode I fracture behaviors of CNT/epoxy/basalt multi-scale composites were

* Corresponding authors. Tel.: +82 31 201 2565; fax: +82 31 202 6693.
E-mail addresses: rheeky@khu.ac.kr (K.Y. Rhee), sjpark@inha.ac.kr (S.J. Park).

1359-8368/$ - see front matter © 2012 Elsevier Ltd. All rights reserved.
doi:10.1016/j.compositesb.2011.12.007

investigated. Flexural and fracture tests were performed on acid-treated and silane-treated CNT/basalt/epoxy multi-scale composites. The fracture surfaces of the composites were examined via field emission scanning electron microscopy (FESEM) to determine the dispersion of CNTs and fracture mechanisms with respect to the surface modification of the CNTs.

2. Experimental

2.1. Material

The carbon nanotubes and reinforcing fibers used in this study were multi-walled carbon nanotubes (MWCNTs, CM-95, Hanhwa Nanotech, Korea) prepared by chemical vapor deposition and woven basalt fiber (EcoB4-F260, Secotech, Korea). Both fibers had an area density of 260 g/m^2. The epoxy used was the diglycidyl ether of bisphenol A (YD-115, Kukdo Chemical, Korea), and the curing agent was polyamidoamine (G-A0533, Kukdo Chemical, Korea). The reagents used for the acid treatment were nitric acid (60–62%, Junsei Chemical, Japan), sulfuric acid (95%, Junsei Chemical), acetone (99.5%, Dae Jung Chemical, Korea), and ethanol (99.5%, Aldrich, USA). The silane functionalization agent was 3-aminopropyltriethoxysilane with a purity of 99% (Aldrich, USA).

2.2. Surface treatment of CNTs

The acid and silane treatments of CNTs were performed according to the procedure described in Fig. 1.

2.3. Fabrication of multi-scale CNT/epoxy/basalt composites

The fabrication process of multi-scale CNT/epoxy/basalt composites was as follows. Epoxy resin mixed with hardener (2:1 v/v) was prepared using 1 wt.% oxidized and silanized CNTs. Eight plies of basalt fabric were then impregnated into the matrix, and the multi-scale composites were cured in an autoclave (ISA-CA30, Ilshin Co., Korea) at 3 kg$_f$/cm^2 and 130 °C for 2 h.

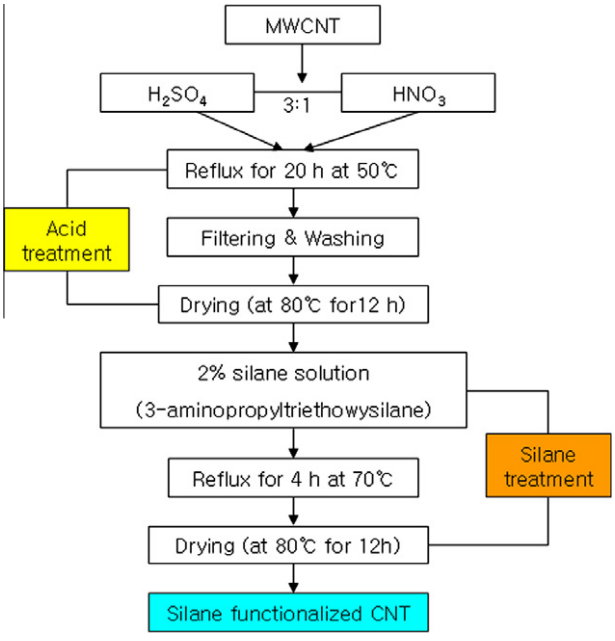

Fig. 1. Flow chart of oxidization and silanization process.

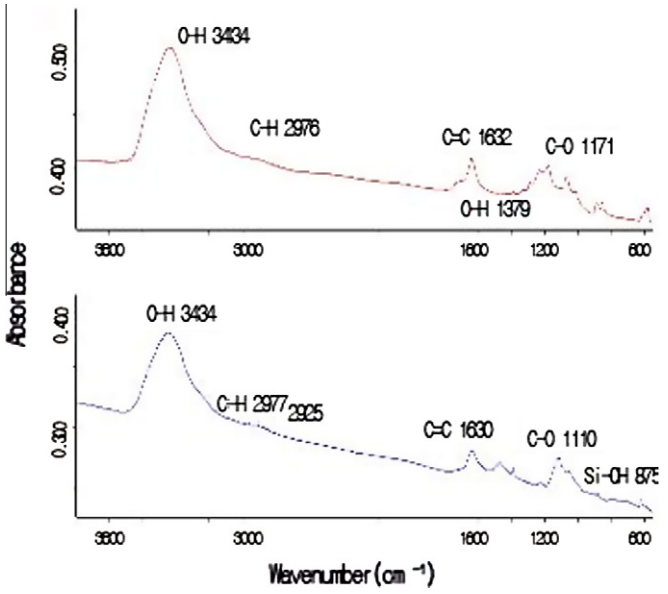

Fig. 2. FT-IR spectrum of (a) acid-treated and (b) silane-treated carbon nanotubes.

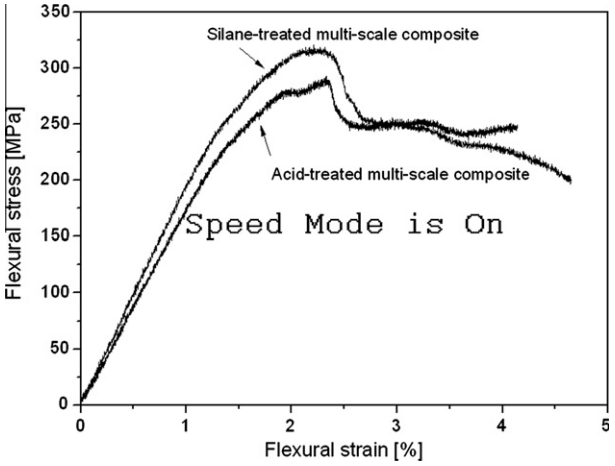

Fig. 3. Stress–strain curves obtained from flexural test of acid-treated and silane-treated multi-scale composites.

2.4. Flexural and fracture tests

Flexural tests were performed with an Instron universal testing machine (Model: 8801) according to the ASTM D-790 [23] standard in a three-point bending mode and at a cross-head rate of 1.0 mm/min using 60 × 25 × 2.4 mm^3 specimens. Mode I fracture tests were performed using double cantilever beam (DCB) fracture specimens (width 25 mm and length 200 mm). An initial delamination was performed by inserting a 50 mm kapton film (thickness 13 μm) between the fourth and fifth plies. One side of the specimen was coated with correction fluid, and lines were drawn 1 mm apart to measure the delamination length. Displacement was controlled at a loading rate of 0.5 mm/min in the fracture tests performed according to ASTM D 5528-01 using a universal testing machine at room temperature [24]. After the initial delamination increased to a certain extent, the applied displacement was reduced and then increased again to cause further delamination. This process was repeated more than 10 times until the delamination increased to greater than 30 mm. Five flexural and fracture tests were performed to ensure the reliability of the test results.

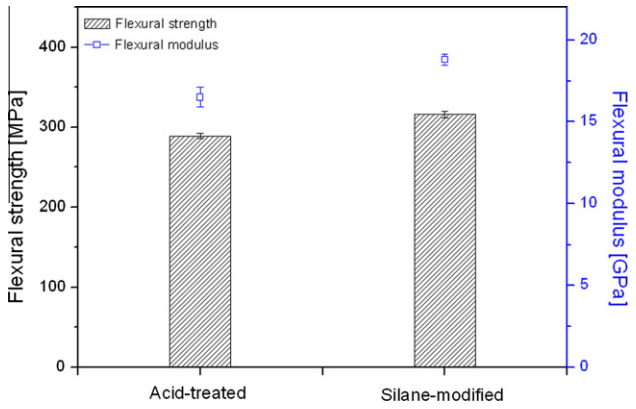

Fig. 4. Comparison of flexural strength and flexural modulus between acid-treated and silane-treated multi-scale composites.

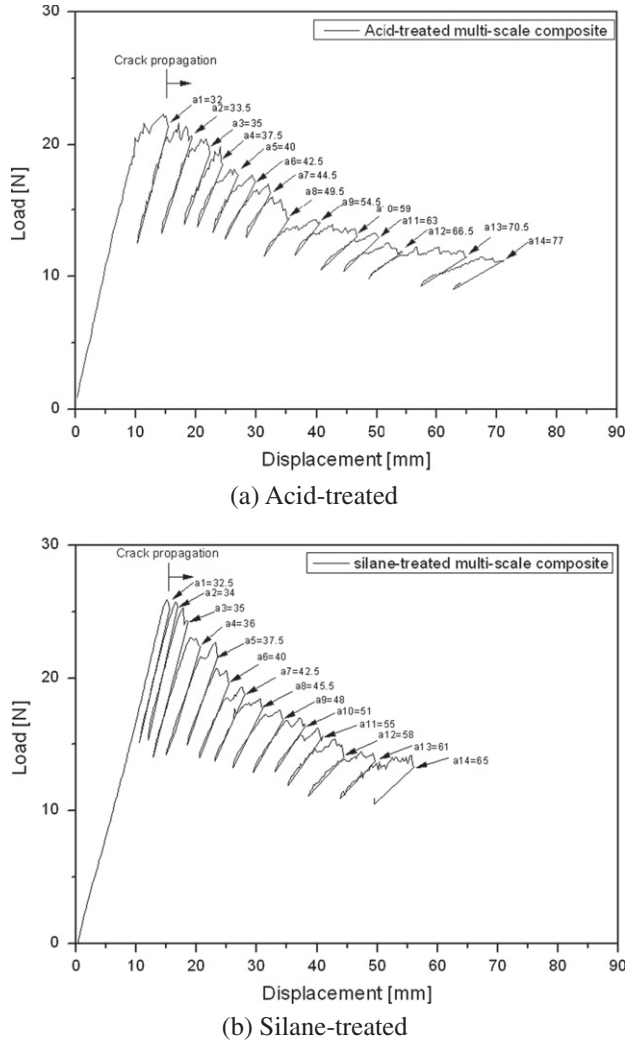

Fig. 5. Load–displacement curves of (a) acid-treated and (b) silane-treated multi-scale composites.

2.5. Determination of mode I fracture toughness

Mode I fracture toughness G_{Ic} was determined from the compliance calibration method as follows:

$$G_{IC} = \frac{nP_{cr}\delta}{2ba} \quad (1)$$

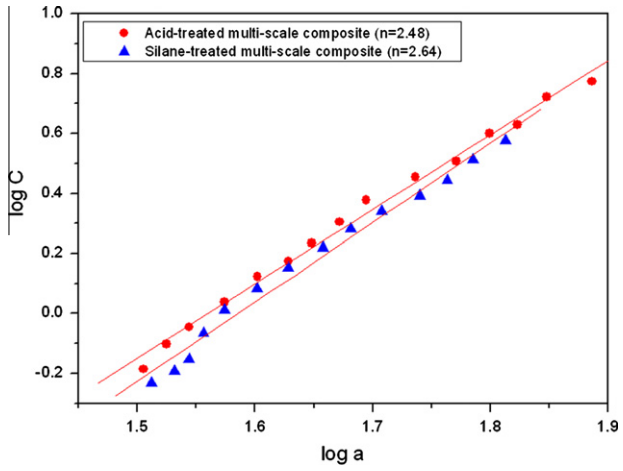

Fig. 6. Comparison of n values in $\log C$–$\log a$ scale.

where a represents the crack length, b is the specimen width, δ is the load-point displacement, and P_{cr} is the fracture load. The n value in Eq. (1) represents a slope in the plot of corrected compliance versus crack length on a log–log scale.

3. Results and discussion

FT-IR analysis was performed to determine the chemical changes on the surface of CNT due to the silane treatment. Fig. 2 shows the FT-IR spectra of the acid-treated and silane-treated CNTs. As shown in Fig. 2a, the oxidized CNTs showed carboxylic group (—COOH) vibrations of stretching C=O at 1699 cm^{-1} and C—O at 1171 cm^{-1} [25]. The peak at 3440 cm^{-1} was from the OH groups on the surface, and the peak at 1379 cm^{-1} was due to the OH bending deformation in —COOH. Therefore, the CNTs were oxidized, and —OH and —COOH groups were present. For the silane-treated CNTs, as shown in Fig. 2b, the characteristic peak is observed at 875 cm^{-1} due to Si—OH [26]. This confirmed the reaction of 3-aminopropyltriethoxysilane with the oxidized CNTs.

Load–displacement curves of flexural tests were determined to investigate the effects of silane treatment on the flexural properties of CNT/epoxy/basalt multi-scale composites. Fig. 3 shows the flexural stress–strain curves of acid-treated and silane-treated CNT/epoxy/basalt multi-scale composites. As shown in the figure, the flexural load increased linearly with displacement up to the

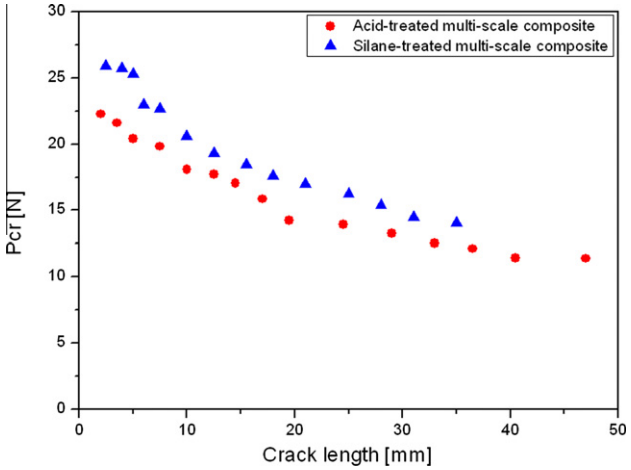

Fig. 7. Comparison of P_{cr} as a function of crack length.

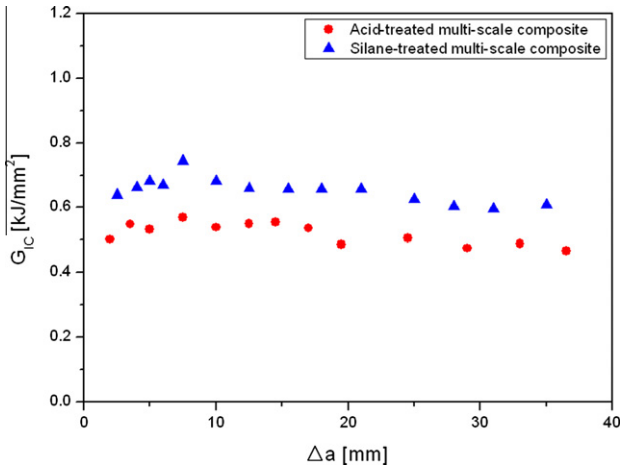

Fig. 8. Comparison of G_{Ic} values as a function of crack length; (a) acid-treated and (b) silane-treated multi-scale composites.

maximum flexural stress for both composites. Fig. 4 compares the flexural strength of the silane-treated CNT/epoxy/basalt multi-scale composites with that of acid-treated CNT/epoxy/basalt multi-scale composites; the flexural strength in each case was defined as the maximum stress in the corresponding stress–strain curve. As shown in the figure, the flexural strength and flexural modulus of the CNT/epoxy/basalt multi-scale composites were slightly improved, ~10% and ~14%, respectively, compared to those of the acid-treated CNT/epoxy/basalt multi-scale composites, by the silane treatment of the CNTs. The flexural modulus in each case was determined by measuring the slope in the linear region of the corresponding load–displacement curve. The figure shows that the flexural strength and flexural modulus of CNT/epoxy/basalt multi-scale composites were affected by the silane treatment of CNTs.

Specifically, the flexural modulus of the silanized CNT/epoxy/basalt multi-scale composites was ~14% greater than that of the acid-treated CNT/epoxy/basalt multi-scale composites.

As can be seen in Eq. (1), compliance and fracture load should be determined as functions of crack length in order to calculate the fracture toughness with the compliance calibration method.

Fig. 5 compares typical mode I load–displacement curves along with the crack increase for acid-treated and silane-treated CNT/epoxy/basalt multi-scale composites. As shown in the figure, non-linear fracture behavior was observed for both composites before the load reached its maximum, and the displacement did not completely return to zero.

The variations in compliance with crack propagation for both composites were determined based on the load–displacement curves, where the compliance for each crack length was determined by measuring the inverse slope of the corresponding unloading line. Fig. 6 shows the variations in compliance with crack increase on a log–log scale for the acid-treated and silane-treated CNT/epoxy/basalt multi-scale composites. C and a in Fig. 6 represent the compliance and crack length, respectively. The figure shows that, although the difference is not significant, the compliance of the silane-treated specimen is smaller than that of the acid-treated specimen at the same crack length. The figure also shows that a linear relationship exists between log C and log a for each specimen, and the values of n that were determined as the slopes of the plots were different between the two specimens. The n values of acid-treated and silane-treated specimens were 2.4 and 2.6, respectively.

The fracture load P_{cr} was determined as a function of crack length, where P_{cr} was determined as the value of the maximum load on the corresponding load–displacement curve. Fig. 7 shows the variations in fracture load during the slow stable crack increase for the acid-treated and silane-treated specimens. For both specimens, fracture load decreased with increasing crack length. Contrary to the compliance requirements, P_{cr} of the silane-treated specimen was greater than that of the acid-treated sample at the same crack length. This indicates that the silane treatment of CNTs increases the adhesion strength between the layers of CNT/epoxy/basalt multi-scale composites.

The variation in the mode I fracture toughness G_{Ic} with the crack increment was determined from Eq. (1) using the n values in Fig. 6 and the P_{cr} values in Fig. 7.

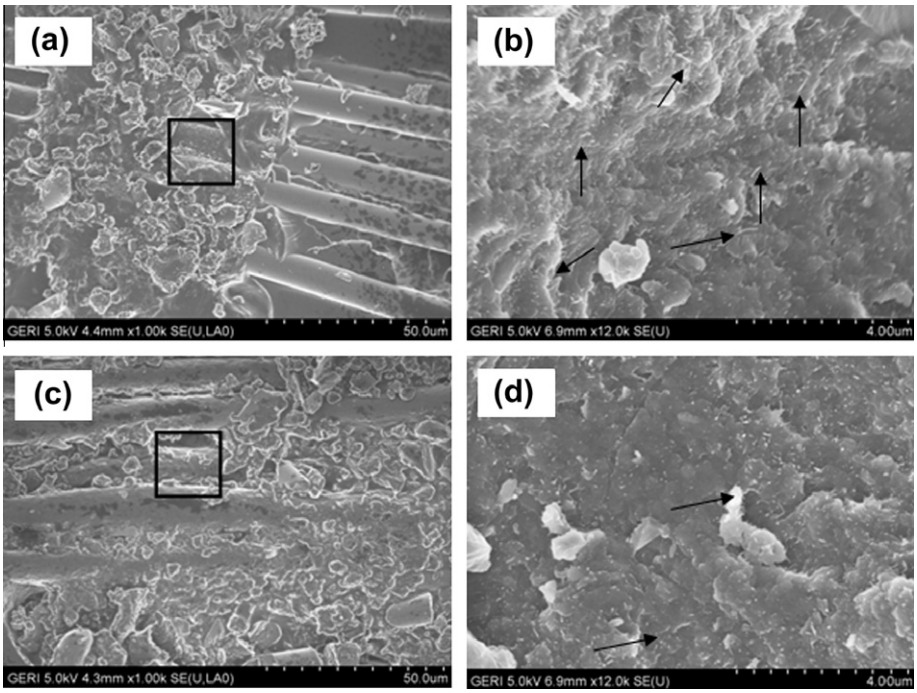

Fig. 9. SEM images of fracture surfaces (a) acid-treated and (c) silane-treated multi-scale composites; (b), (d) are magnified images of boxed region in (a), (c), respectively.

Fig. 8 shows a comparison of the variation in G_{Ic} with crack length for the silane-treated specimen with that for the acid-treated specimen. As shown in the figure, G_{Ic} varies in a limited range with crack length for both specimens. The figure also shows that G_{Ic} of the silane-treated specimen was greater than that of the acid-treated specimen at the same crack length. Specifically, the averaged values of G_{Ic} for acid-treated and silane-treated CNT/epoxy/basalt multi-scale composites were 0.5 kJ/mm^2 and 0.7 kJ/mm^2, respectively.

That is, mode I fracture toughness was improved about 40% by the silane modification of CNTs. Considering that the compliance of the silane-treated specimen is smaller than that of the acid-treated specimen, it can be inferred that the improvement in G_{Ic} was due to the improved fracture load. The primary reason why fracture toughness was improved by surface-treatment of CNTs was that interfacial bonding strength between CNTs and the epoxy matrix was improved, which leads to a suppression of debonding at the interface and crack propagation. Therefore, fracture toughness was improved as CNTs were surface-treated with 3-aminopropyltriethoxysilane.

SEM analysis was performed on the fracture surfaces of the acid-treated and silane-treated CNT/epoxy/basalt multi-scale composites after the fracture tests. Fig. 9a shows the fracture surface of the acid-treated specimen, and Fig. 9b shows the magnified image of the boxed region in Fig. 9a. As shown in the figures, the fracture surface was relatively clean, and some basalt fibers were removed from the epoxy matrix. The figure also shows that CNTs were partially agglomerated and unimpregnated in the epoxy matrix, whereas partially removed CNTs were observed in the magnified image (indicated by arrows). The clean surfaces of basalt fibers with debonded CNT-reinforced epoxy resin occurred because the load transfer to the basalt fibers increased due to agglomeration and bad interfacial interaction between the CNTs and epoxy matrix. Fig. 9c shows the fracture surface of the silane-treated specimen, and Fig. 9d shows the magnified image of the boxed region in Fig. 9c. In comparison to the acid-treated specimen, basalt fibers were well harmonized with the epoxy matrix, and CNTs were well dispersed and impregnated in the epoxy matrix. The figures also show that the CNT removal decreased in the epoxy matrix. The epoxy-rich region on the basalt fibers occurred due to homogeneous load support of basalt fibers by improved dispersibility and interfacial interaction of CNTs in the epoxy matrix.

4. Conclusions

In this study, we investigated the effects of CNT modification with silane on the flexural and fracture behaviors of carbon nanotube modified epoxy/basalt composites. The conclusions obtained from this study are as follows. The flexural modulus and strength of silane-treated CNT/epoxy/basalt multi-scale composites were ~10% and ~14% greater, respectively, than those of acid-treated CNT/epoxy/basalt multi-scale composites. The fracture toughness G_{Ic} of silane-treated CNT/epoxy/basalt multi-scale composites was ~40% greater than that of acid-treated CNT/epoxy/basalt multi-scale composites. The silane modification of CNTs increased dispersibility and interfacial bonding between the CNTs and epoxy resin and supported the homogeneous load transfer capacity of basalt fibers. This causes the silane-treated CNT/epoxy/basalt multi-scale composites to have higher flexure and fracture properties than those of acid-treated CNT/epoxy/basalt multi-scale composites.

Acknowledgment

This research was supported by Basic Science Research Program through the National Research Foundation of Korea (NRF) funded by the Ministry of Education, Science and Technology (2010-0023106).

References

[1] Czigány T. Basalt fiber reinforced hybrid polymer composites. Mater Sci Forum 2005;473:59–66.
[2] ÖZTÜRK S. The effect of fibre content on the mechanical properties of hemp and basalt fibre reinforced phenol formaldehyde composites. J Mater Sci 2005;40:4585–92.
[3] Ronkay F, Czigány T. Development of composites with recycled PET matrix. Polym Adv Technol 2006;17:830–4.
[4] Liu Q, Shaw MT, Parnas RS, McDonnell AM. Investigation of basalt fiber composite mechanical properties for applications in transportation. Polym Compos 2006;27:41–8.
[5] Choudhury A, Kar P. Doping effect of carboxylic acid group functionalized multi-walled carbon nanotube on polyaniline. Composites Part B 2011;42:1641–7.
[6] Gojny FH, Nastalczyk J, Roslaniec Z, Schulte K. Surface modified multi-walled carbon nanotubes in CNT/epoxy-composites. Chem Phys Lett 2003;370:820–4.
[7] Feng QP, Yang JP, Fu SY, Mai YW. Synthesis of carbon nanotube/epoxy composite films with a high nanotube loading by a mixed-curing-agent assisted layer-by-layer method and their electrical conductivity. Carbon 2010;48:2057–62.
[8] Park OK, Kim NH, Yoo GH, Rhee KY, Lee JH. Effects of the surface treatment on the properties of polyaniline coated carbon nanotubes/epoxy composites. Composites Part B 2010;41:2–7.
[9] Geng Y, Liu MY, Li J, Shi XM, Kim JK. Effects of surfactant treatment on mechanical and electrical properties of CNT/epoxy nanocomposites. Composites Part A 2008;39:1876–83.
[10] Fu SY, Feng XQ, Lauke B. Effects of particle size, particle/matrix interface adhesion and particle loading on mechanical properties of particulate-polymer composites. Composites Part B 2008;39:933–61.
[11] Zhao X, Ye L. Structure and mechanical properties of polyoxymethylene/multi-walled carbon nanotube composites. Composites Part B 2011;42:926–33.
[12] Thostenson ET, Li WZ, Wang DZ, Ren ZF, Chou TW. Carbon nanotube/carbon fiber hybrid multiscale composites. J Appl phys 2002;91:6034–7.
[13] Davis DC, Whelan BD. An experimental study of interlaminar shear fracture toughness of a nanotube reinforced composite. Composites Part B 2011;42:105–16.
[14] Romhány G, Szebényi G. Interlaminar crack propagation in MWCNT/fiber reinforced hybrid composites. eXPRESS Poly lett 2009;3:145–51.
[15] Zhang FH, Wang RG, He XD, Wang C, Ren LN. Interfacial shearing strength and reinforcing mechanisms of an epoxy composite reinforced using a carbon nanotube/carbon fiber hybrid. J Mater Sci 2009;44:3574–7.
[16] Kepple KL, Sanborn GP, Lacasse PA, Gruenberg KM, Ready WJ. Improved fracture toughness of carbon fiber composite functionalized with multi walled carbon nanotubes. Carbon 2008;46:2026–33.
[17] Lin GM, Xie GY, Sui GX. Hybrid effect of nanoparticles with carbon fibers on the mechanical and wear properties of polymer composites. Composites Part B 2012;43:44–9.
[18] Bekyarova E, Thostenson ET, Yu A, Kim H, Gao J, Tang J, et al. Multiscale carbon nanotube–carbon fiber reinforcement for advanced epoxy composites. Langmuir 2007;23:3970–4.
[19] Qiu JJ, Zhang C, Wang B, Liang R. Carbon nanotube integrated multifunctional multiscale composites. Nanotechnology 2007;18:275708.
[20] Yamamoto T, Miyauchi Y, Motoyanagi J, Fukushima T, Aida T, Kato M, et al. Improved bath sonication method for dispersion of individual single-walled carbon nanotubes using new triphenylene-based surfactant. Jpn J Appl Phys 2008;47:2000–4.
[21] Chen Y, Conway MJ, Fitzgerald JD. Carbon nanotubes formed in graphite after mechanical grinding and thermal annealing. Appl Phys A 2003;76:633–6.
[22] Lee JH, Rhee KY, Park SJ. The tensile and thermal properties of modified CNT-reinforced basalt/epoxy composites. Mater Sci Eng A 2010;527:6838–43.
[23] ASTM D 790. Standard test methods for flexural properties of unreinforced and reinforced plastics and electrical insulating materials.
[24] ASTM D 5528-01. Standard test method for Mode I interlaminar fracture toughness of unidirectional fiber-reinforced polymer matrix composites.
[25] Kuznetsova A, Douglas D, Namneko V, Yates Jr JT, Liu J, Smalley RE. Enhancement of adsorption inside of single-walled nanotubes: opening the entry ports. Chem Phys Lett 2000;321:292–6.
[26] Satyanarayana N, Xie X, Rambabu B. Sol–gel synthesis and characterization of the Ag_2O—SiO_2 system. Mater Sci Eng B 2000;72:7–12.